



Electrocatalytic Determination of Hydroxychloroquine Using Sodium Dodecyl Sulphate Modified Carbon Nanotube Paste Electrode

P. A. Pushpanjali¹ · J. G. Manjunatha¹ · N. Hareesha¹ · T. Girish¹ · Abdullah A. Al-Kahtani² · Ammar Mohamed Tighezza² · Narges Ataollahi³

Accepted: 31 December 2021

© The Author(s), under exclusive licence to Springer Science+Business Media, LLC, part of Springer Nature 2022

Abstract

Selective, sensitive, easy, and fast voltammetric techniques were developed for the analysis of Hydroxychloroquine (HCQ). These analysis were carried out at sodium dodecyl sulphate modified carbon nanotube paste electrode (SDSMCNTPE) using an aqueous 0.2 M phosphate buffer solution as supporting electrolyte. The field emission-scanning electron microscopy, cyclic voltammetry (CV), and electrochemical impedance spectroscopy were used for material characterization. A minute quantity of the SDS surfactant was sufficient to convey an outstanding electrocatalytic action to the electrochemical oxidation nature of HCQ. The HCQ molecule parades only electrochemical oxidation (irreversible) with the transfer of two electrons. The detection of HCQ was carried out through CV method at SDSMCNTPE and bare carbon nanotube paste electrode (BCNTPE). The corresponding analytical curve offered a decent linear nature in the considered HCQ concentration range (10–40 μM) and the detection limit was found to be 0.85 μM . The significant peak to peak split-up was observed between HCQ and interferents with a decent sensitivity and stability. The SDSMCNTPE to be an approachable electrode for the usage in the examination of HCQ independently and in the presence of paracetamol (PC) and ascorbic acid (AA). Thus, they were used to determine HCQ in pharmaceutical formulations and the results that showed good agreement with comparative methods. Furthermore, a mechanism for HCQ electro-oxidation was proposed.

Keywords Hydroxychloroquine · Paracetamol · Ascorbic acid · Carbon nanotube sensor · Electroanalysis

1 Introduction

HCQ is utmost commonly consumed as a first-line medication for auto immune based diseases in patients like systemic lupus erythematosus and rheumatoid arthritis and has increased wide media attention as a promising antiviral drug for usage versus severe acute respiratory syndrome (which causes COVID-19) [1–7]. Unfortunately, the origination of research on HCQ has preceded to misperception in

the rheumatological community concerning the protection consequences of HCQ in its conventional customs. Medical examinations on COVID-19 and broadcasting courtesy have directed to communal awareness based on HCQ [7–9]. Due to the extensive usage of this medication, numerous analytical methods have been operated for the analysis of HCQ involving extraction ensued through nonaqueous titrimetric approach [10], assay-based methods, HPLC [11], fluorescence [12], ultraviolet spectroscopy [13], spectrophotometry [14], and tandem mass spectrometry [15]. Nonetheless, these analytical approaches show a variety of difficulties like costly and time-consuming instrumentation, complicated sample pre-treatment processes, necessity of skilled analyst, more consumption of compounds and high detection limit. Electrochemical approaches frequently have numerous benefits over these conventional methods like, easy and lesser price instrumentation, less consumption of analyte, high detection ability and rapid investigation time [16–34]. Nanotechnology has become very popular in the sensor field in recent times due to the variety of profiles, dimensions

✉ J. G. Manjunatha
manju1853@gmail.com

¹ Department of Chemistry, FMKMC College, Constituent College of Mangalore University, Madikeri, Karnataka, India

² Chemistry Department, College of Science, King Saud University, P. O. Box 2455, Riyadh 11451, Saudi Arabia

³ Department of Civil, Environmental and Mechanical Engineering, University of Trento, Via Mesiano, 77, 38123 Trento, Italy

and conformations. Nowadays, carbon based nano-materials like carbon-based nanoparticles, carbon nanotubes, carbon nano-composites, carbon dots and carbon nano-wires are too significant in various fields like sensors, supercapacitors, pharmaceutical and biological samples analysis and so on. In that, carbon nanotubes show very important applications such as larger surface area, more active sites, good electrical conductivity, high stability, and fine analyzing ability for the examination of medicinal samples and which might afford a significant and achievable platform for the electroanalysis and particularly in the formulation of electroanalytical sensor materials [35–45]. Corresponding to the overhead points, the application of carbon nanotubes is important to develop an electrochemical sensor with high sensitivity and the reduction of over potential based on modifying agents. In the present scrutiny, we developed the SDSMCNTPE for the analysis of HCQ in phosphate buffer solution (PBS) of pH 6.5 in presence of PC and AA molecules based on CV methodology. The high electro-catalytic capacity of SDSMCNTPE for the HCQ oxidation was verified in both real and commercial HCQ samples. A deep literature review guided that no effort has been completed on HCQ analysis at SDSMCNTPE. Thus, the purpose of this analysis was focused on the study and optimization of experimental circumstances for the HCQ detection in tablet sample by means of SDSMCNTPE as a fast, simple and sensitive tool.

2 Experimental

2.1 Materials and Reagents

SDS, PC, AA and sodium salts of monobasic (NaH_2PO_4) and dibasic phosphate (Na_2HPO_4) were got from HiMedia chemicals. CNTs are obtained from Sisco Research Laboratory. $\text{K}_4[\text{Fe}(\text{CN})_6]$ was bought from Sigma-Aldrich. All the used chemicals are of analytical reagent grade with 95–99.5% of purity. Distilled water was utilized during the preparation of all the chemical solutions. The required solutions of HCQ (0.1 mM), PC (1.0 mM) and AA (1.0 mM) are prepared by suspending the essential measure of corresponding solute in distilled water.

2.2 Instruments

CV and EIS are carried out with an electroanalytical instrument of model CHI-6038E (CH Instruments, USA). The electrochemical cell was constituted to this work attached by three electrodes, SDSMCNTPE and BCNTPE as the working, calomel electrode (Hg_2Cl_2 saturated with KCl) as reference and a Pt wire as counter electrode. The pH meter (Equiptronics) was used for adjusting pH values. This

overall analysis was accomplished at the lab temperature of $25(\pm 2)^\circ\text{C}$.

2.3 Preparation of Surfactant Modified Carbon Electrodes

The BCNTPE was prepared according to the procedure described by our previous works [46, 47]. We describe a trouble-free process to get SDS surfactant immobilized CNTPE. The scheme is constructed on the accumulation of surfactant molecules on the surface of CNTPE. Initially, the electrochemical response of HCQ at SDSMCNTPE is measured. SDS was immobilized on the surface of CNTPE by surface modification method using micropipette and the electrode was rinsed with distilled water.

3 Results and Discussion

3.1 Material Characterization

The response of the electrochemical sensor was related to its physical morphology. Typical FE-SEM imageries of distinctive electrode materials were revealed in Fig. 1. The field emission-scanning electron microscopy (FE-SEM) image of BCNTPE surface (Fig. 1a) was categorized through a dense tube-like shape which are detached and erratically arranged. Although, the FE-SEM picture of SDSMCNTPE showed vastly unlike morphology associated to BCNTPE, after the SDS immobilization on BCNTPE. Here, SDS was dispersed on the exterior of the CNTPE surface with consistent formation (Fig. 1b), representing that the SDS was efficaciously accumulated on CNTPE and promotes the electron transfer in HCQ oxidation.

3.2 Effect of Surfactant Concentration

The impact of boosted concentration of SDS in the range from 5.0 to 25.0 μL at CNTPE surface for the HCQ oxidation was examined by recording CVs and the obtained responses are shown in Fig. 2a. Here, the oxidation current of HCQ molecule in PBS at different concentration of SDS on CNTPE is varied due the molecular interactions among SDS and HCQ. Also, from Fig. 2b, the oxidation current of HCQ was higher at 10.0 μL of SDS than other SDS concentrations like 5.0, 15.0, 20.0 and 25.0 μL . This effect is most possibly due to the result of critical accumulation concentration of SDS on CNTPE surface. Then, 10.0 μL of SDS concentration was operated as finest concentration for highly sensitive HCQ oxidation throughout the experiment.

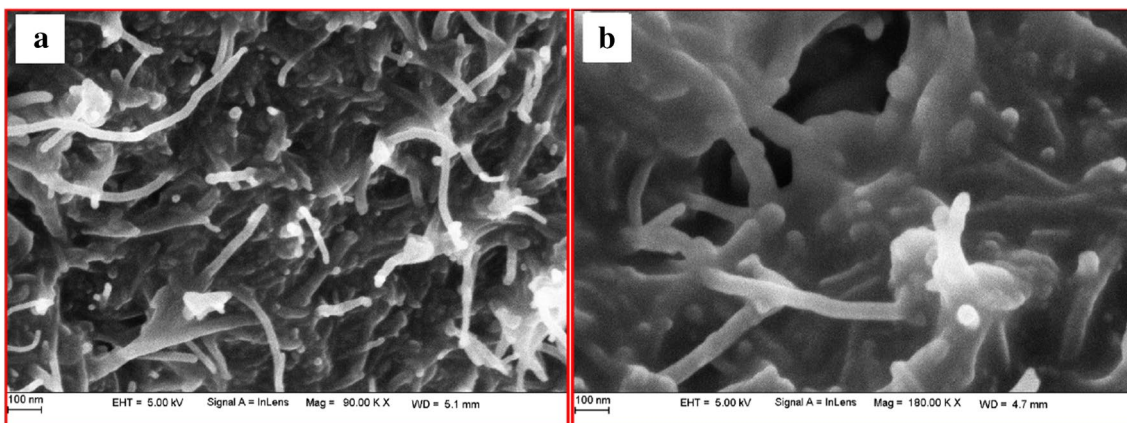


Fig. 1 FE-SEM pictures of **a** BCNTPE and **b** SDSMCNTPE

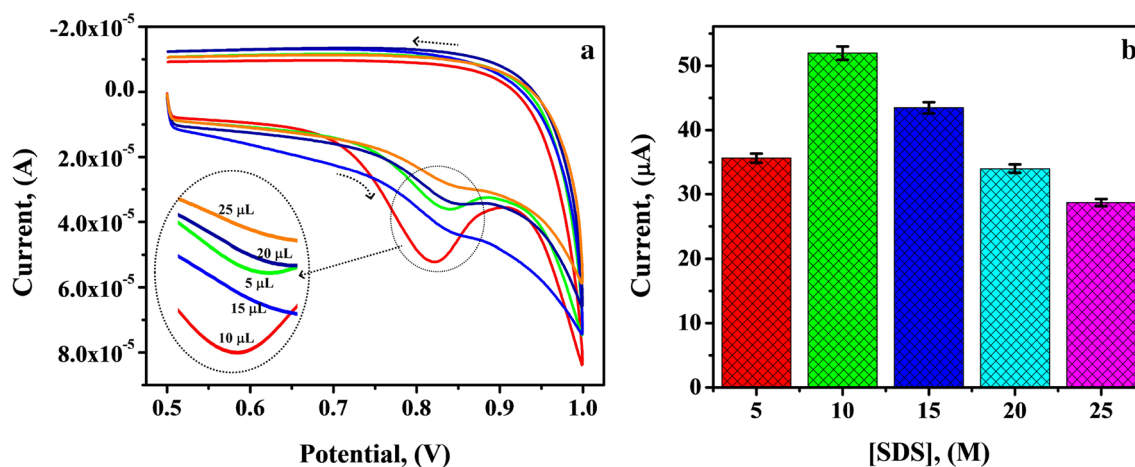


Fig. 2 **a** CVs of 0.1 mM HCQ in 0.2 M PBS at the surface of CNTPE with different SDS concentrations in the range from 5.0 to 25.0 μL . **b** Plot of concentration of SDS vs. peak current of HCQ

3.3 Electrochemical Impedance Spectroscopy

Electrochemical impedance spectroscopy (EIS) is the significant tool for quantifying the conductance and resistance of the used working electrode materials at the interface of PBS and electrode surface. The EIS outcomes for BCNPE (a) and SDSMCNTPE (b) are explicated through the utilization of Nyquist plots shown in Fig. 3. The EIS was accomplished for $\text{K}_4[\text{Fe}(\text{CN})_6]$ (1.0 mM) in KCl (0.10 M) having the potential of 0.10 V. From the Nyquist plots (a, b), the BCNTPE semicircle radius was higher than SDSMCNTPE, which specified that the charge transfer resistance (R_{ct}) of SDSMCNTPE is lesser as compared to BCNTPE. This obtained data shows that, the conductance of SDSMCNTPE is more with more active sites and this is probably due to the strong interaction of SDS and CNTPE surface [46].

3.4 The pH Effect

The impact of pH is the important feature to get the expectant solution pH shows superior oxidation peak current for HCQ. The solution pH impacts the oxidation nature of HCQ at SDSMCNTPE with respect to peak current and potential. The influence of solution pH was analyzed for the oxidation of HCQ in different pHs in the range from 6.0 to 8.0 on SDSMCNTPE via CV technique at 0.1 V/s scan rate. The CVs for 1.0 mM HCQ at SDSMCNTPE show the movement of oxidation peak potential towards the negative direction as the intensification of pH of PBS (Fig. 4a). The pH vs. E_{pa} relation parades a good linearity (Fig. 5b) with the linear regression equation is $E_{pa}(\text{V}) = 1.2847 - 0.0720 \text{ pH}$ (V/pH) ($R = 0.9931$). Here, the slope value (-0.070 V/pH) is nearer to the hypothetical value which describes that the oxidation nature of HCQ is proceeds over the transport of alike

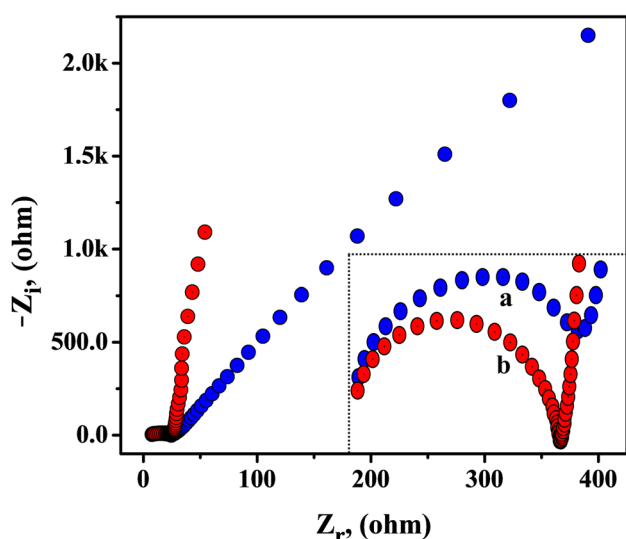


Fig. 3 EIS plots of BCNTPE (a) and SDSMCNTPE (b)

number of protons and electrons [48–50]. Moreover, Fig. 5b reveals that, the 6.5 pH imparts higher oxidation current of HCQ, hence this was selected as optimal pH for this study.

3.5 Effect of Scan Rate on HCQ at SDSMCNTPE

The scan rate influence on the oxidation reaction of 0.1 mM HCQ (with 0.2 M PBS having pH of 6.5) at SDSMCNTPE was studied via CV method by varying the scan rate from 0.10 to 0.30 V/s having the potential difference from 0.5 to 1.0 V. The CVs of HCQ in Fig. 5a, the oxidation current of each CV sequence is enhanced with small alteration in the potential towards the positive way as the rise of scan rate. Figure 5b specifies the graph log oxidation current ($\log I_{pa}$) vs. log scan rate ($\log v$) influencing a good

linear agreement with the linear regression equation is $\log(I_{pa}, \mu A) = 1.5141 + 0.8247 \log(v, V/s)$ ($R = 0.9902$). The obtained slope value suggests that, the electro-catalytic action of SDSMCNTPE for the oxidation response of HCQ was completed by the adsorption-controlled pathway [51–53].

3.6 Electrochemical Response of HCQ

The electrochemical oxidation response of 0.1 mM HCQ (presence and absence) in 0.20 M PBS with pH 6.5 on SDSMCNTPE and BCNTPE was evaluated by utilizing CV method at the potential interval of 0.5–1.0 V at the scan rate of 0.1 V/s. The CVs in Fig. 6 reveals that, the HCQ absence (blank) in 0.2 M PBS having pH 6.5 at SDSMCNTPE display no electrochemical reply. Nevertheless, the CVs for HCQ at SDSMCNTPE and BCNTPE presents the electrochemical reaction with comparable oxidation peak current and potentials for HCQ. The BCNTPE discloses a very low electrochemical oxidation response for HCQ with smaller peak current compared to the SDSMCNTPE. This data explains that, the SDSMCNTPE shows higher sensitivity with enhanced electro-catalytic action for the oxidation of HCQ with quicker rate of proton and electron movement than at BCNTPE. Also, the electrochemical response of HCQ at SDSMCNTPE was observed to be enhanced by five fold compared to that noticed at BCNTPE. This could be due to the presence of higher surface area. The possible oxidation reaction mechanism of HCQ on SDSMCNTPE is shown in Fig. 6b [54].

3.7 Electroactive Surface Area

CV was implemented for the analysis of active surface area of BCNTPE and SDSMCNTPE based on the

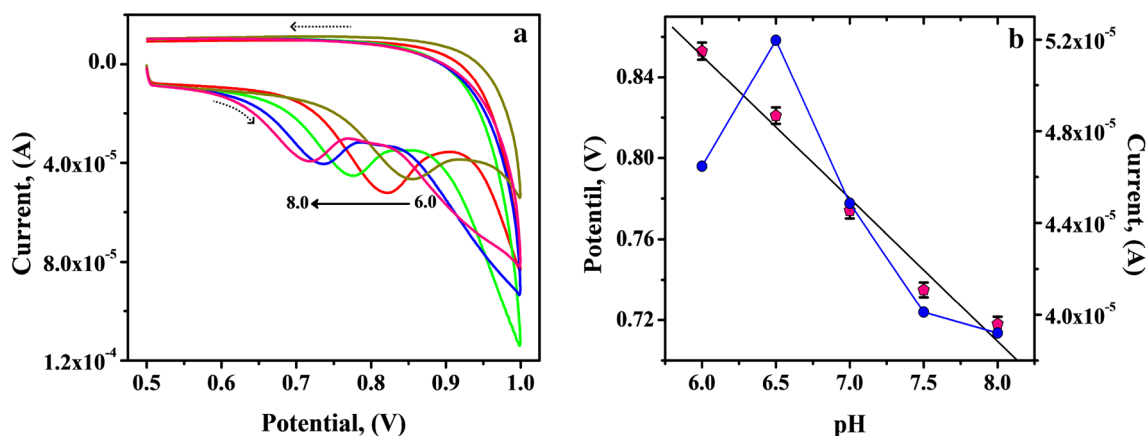


Fig. 4 a CVs of 0.1 mM HCQ at SDSMCNTPE in 0.2 M PBS having altered pHs (6.0–8.0) at the potential gap of 0.5 V–1.0 V with the scan rate of 0.1 V/s. b Plot of pH vs peak potential and pH vs I_{pa}

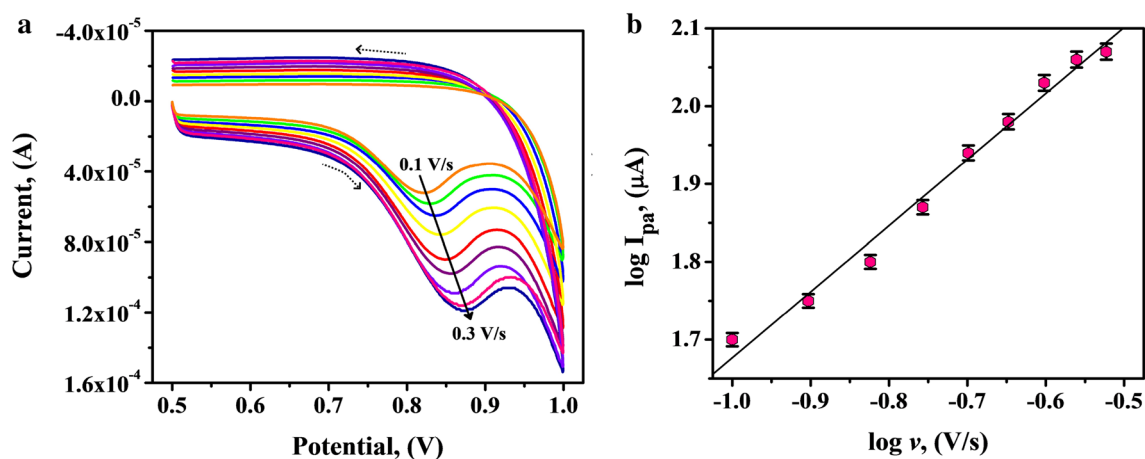


Fig. 5 **a** CVs of 0.1 mM HCQ on SDSMCNTPE in 0.2 M PBS (pH 6.5) based on different scan rate ranging from 0.1 V/s–0.3 V/s with the potential gap of 0.5 V–1.0 V. **b** Plot of log scan rate vs. log peak current

electrochemical response of 1 mM $K_4[Fe(CN)_6]$ in 0.10 M KCl with the scan rate of 0.1 V/s within the potential range of -0.20 to 0.60 V (Fig. 7). The redox peak response of standard analyte at BCNTPE and SDSMCNTPE is displayed in Fig. 7, here SDSMCNTPE shows less redox potential with raised redox current as compared to BCNTPE. This outcome is due to the more active sites, decrease of overpotential and high surface area of the SDSMCNTPE. The active surface area of the operated electrochemical sensors was verified using the Randles–Sevcik equation [33, 55],

$$I_p = 2.69 \times 10^5 n^3/2 A D^{1/2} C v^{1/2} \quad (1)$$

here, A is the electrochemical active surface area (cm^2), I_p is the analyte peak current (A), D is the analyte diffusion coefficient (cm^2/s), n is the number of electrons, v is the scan rate (V/s) and C is the analyte concentration (M). The premeditated electro-active surface area of SDSMCNTPE and BCNTPE are obtained to be 0.044 cm^2 and 0.014 cm^2 , correspondingly.

3.8 Simultaneous Determination of HCQ, PC and AA

The instant examination of HCQ with PC and AA in 0.20 M PBS (pH = 6.5) at BCNTPE and SDSMCNTPE was completed through the operation of CV at 0.1 V/s scan rate (Fig. 8). At BCNTPE, HCQ, PC and AA moieties displays feeble electrochemical action with lesser sensitive peak currents at higher potentials. Nevertheless, at SDSMCNTPE, HCQ, PC and AA parades preminent electrochemical oxidation with greater peak currents and decreased potentials at 0.854, 0.358 and 0.0491 V, respectively. This evidence reveals that, SDSMCNTPE is highly active for the analysis of HCQ in the occurrence of PC and AA with elevated

electrocatalytic achievement and rapid electron transport rate than BCNTPE.

3.9 Calibration Curve

The CVs at SDSMCNTPE (Fig. 9) attained with consecutive addition of different concentration of HCQ at the optimized conditions. The analytical curve shown in Fig. 9a, b, displayed an acceptable linear assortment ranging from 10 to 40 μ M and the regression equation obtained was $I_{pa} = 1.4245 \times 10^{-5} + 0.2929 [HCQ] (M)$, ($R = 0.9995$). The detection limit and quantification limit are calculated using the formulations [56],

$$\text{Detection limit} = 3.0(\text{standard deviation of the blank}) / (\text{slope of analytical curve}) \quad (2)$$

$$\text{Quantification limit} = 10.0(\text{standard deviation of the blank}) / (\text{slope of analytical curve}) \quad (3)$$

The premeditated detection limit and quantification limit values were obtained to be 0.85 and 28.08 μ M, which are decent values as associated to some reported HCQ sensors shown in Table 1 [17, 57]. Also, the electrode sensitivity was calculated based on surface area and slope of the calibration plot and the value was found to be 6.65 M/A/ cm^2 .

3.10 Application to Pharmaceutical Formulation Analysis

The adaptability of SDSMCNTPE was confirmed through the standard addition scheme towards the detection of HCQ in pharmaceutical tablet sample. The HCQ tablet sample

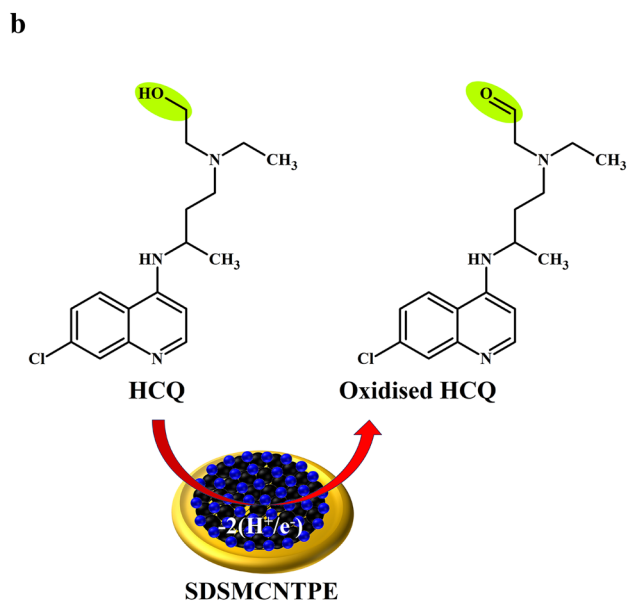
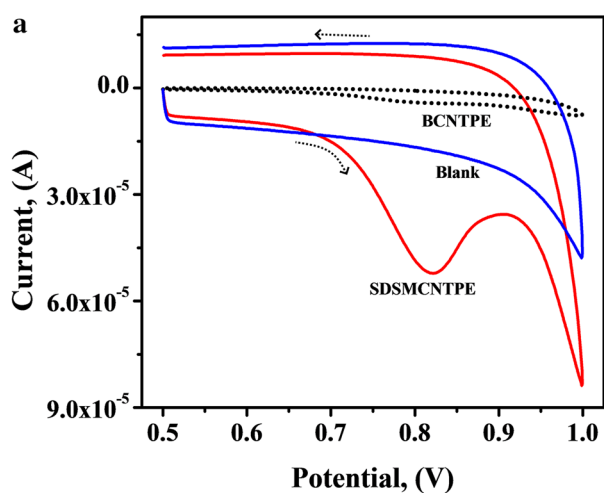


Fig. 6 **a** CVs for the presence and absence (blank) of 0.1 mM HCQ on SDSMCNTPE and BCNTPE in 0.2 M PBS of 6.5 pH at the potential gap of 0.5–1.0 V with the scan rate of 0.1 V/s. **b** Possible oxidation reaction mechanism of HCQ on SDSMCNTPE

was diluted with 0.2 M PBS (pH=6.5) and subjected to the CV method separately having various concentration on SDSMCNTPE at optimized conditions. The HCQ tablet sample at SDSMCNTPE displays a good recovery. The pre-meditated results of percentage recovery of HCQ in tablet are tabulated in Table 2. The achieved results proposed that the SDSMCNTPE is a good substitute for HCQ detection in tablet sample in the occurrence of other interferences.

3.11 Reproducibility and Stability of SDSMCNTPE

The reproducibility of the SDSMCNTPE was assessed by cycling five CV cycles for HCQ (fixed) in PBS at five distinctly prepared SDSMCNTPE electrodes. Here, the prepared

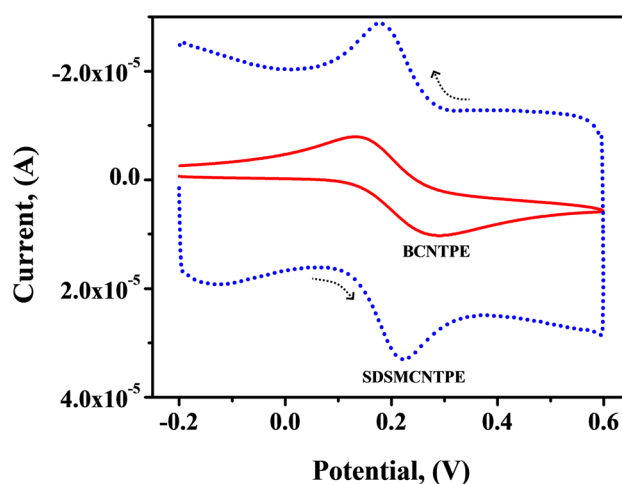


Fig. 7 CVs for 1.0 mM $K_4[Fe(CN)_6]$ in 0.1 M KCl on SDSMCNTPE and BCNTPE at the potential gap of 0.5 V–1.0 V with the scan rate of 0.1 V/s

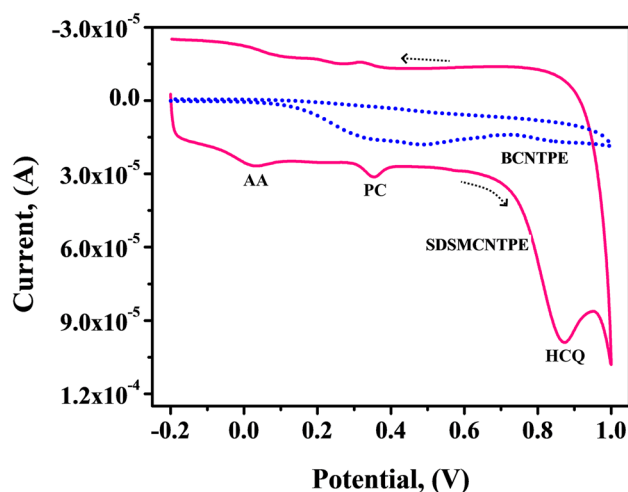


Fig. 8 CVs for HCQ, PC, and AA in 0.2 M PBS at SDSMCNTPE and BCNTPE at the potential gap of – 0.2 to 1.0 V with the scan rate of 0.1 V/s

SDSMCNTPE delivers the relative standard deviation (RSD) of 1.3%, signifying an adequate reproducibility. The stability of SDSMCNTPE for HCQ in PBS was examined via CV technique by keeping the electrode for 2 days in a closed vessel. The retainance of 97.28% of the preliminary current presents the adequate stability of SDSMCNTPE.

4 Conclusion

The current effort suggests a receptive and modest SDSMCNTPE for the examination of HCQ through CV method, which shows the heightened electrode

Table 1 Comparison of previously reported HCQ sensors with the present HCQ sensor

Electrode	Linear range	LOD	Reference
Polymeric membrane electrode	10.0 μ M–10.0 mM	7.90 μ M	[17]
Carbon paste electrode	10.0 μ M–10.0 mM	6.50 μ M	
Coated graphite electrode	71.0 μ M–10.0 mM	18.0 μ M	[57]
SDSMCNTPE	10.0–40.0 μ M	0.85 μ M	Present work

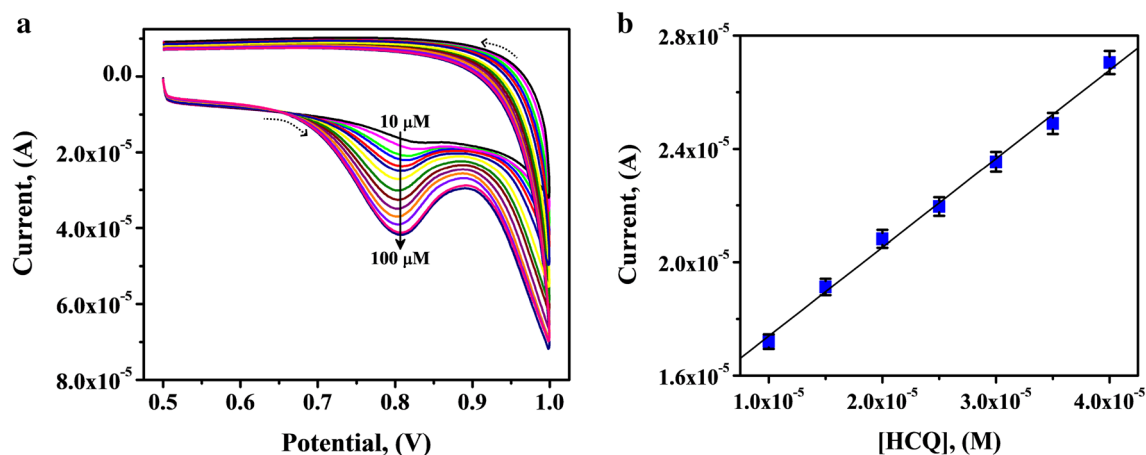

Fig. 9 a CVs for different concentrations of HCQ on SDSMCNTPE in 0.2 M PBS of pH 6.5 at the potential gap of 0.5 V–1.0 V. b Plot of concentration of HCQ vs. peak current

Table 2 Premeditated results of percentage recovery of HCQ in tablet sample

Sample	Added (μ M)	Found (μ M)	Recovery (%)
HCQ tablet sample	20	20.00	100
	25	24.87	99.48
	30	29.50	98.33

conductivity, sensitivity and selectivity. The investigative process has been completely justified by fine linearity, accurateness, sensitivity and reproducibility owing to the improvement of the rate of electron transfer progression with a greater fundamental electroactive surface area and active sites of SDSMCNTPE. This analysis devotes a modest, robust and precise analysis of HCQ and its significance in tablet sample analysis. Additionally, this SDSMCNTPE delivers an exceptionally appropriate and applicable technique for the concurrent detection of HCQ, PC and AA.

Funding P A Pushpanjali grateful to the Researchers Supporting OBC Fellowship, Government of Karnataka, India. Abdullah A, Al-Kahtani and Ammar Mohamed TIGHEZZA grateful to the Researchers

Supporting Project Number (RSP-2021/266), King Saud University, Riyadh, Saudi Arabia.

Declarations

Conflict of interest The author declare no competing interests.

References

- Lammers AJJ, Brohet RM, Theunissen REP et al (2020) Early hydroxychloroquine but not chloroquine use reduces ICU admission in COVID-19 patients. *Int J Infect Dis* 101:283–289. <https://doi.org/10.1016/j.ijid.2020.09.1460>
- Colson P, Rolain JM, Lagier JC, Brouqui P, Raoult D (2020) Chloroquine and hydroxychloroquine as available weapons to fight COVID-19. *Int J Antimicrob Agents* 55:105932
- Devaux CA, Rolain JM, Colson P, Raoult D (2020) New insights on the antiviral effects of chloroquine against coronavirus: what to expect for COVID-19? *Int J Antimicrob Agents* 55:105938
- Chen JJ, Tarantola RM, Kay CN, Mahajan VB (2011) Hydroxychloroquine (plaqueuil) toxicity and recommendations for screening. *Eye Rounds* org. Available from <http://EyeRounds.org/cases/139-plaqueuil-toxicity.htm>. Accessed 14 Sept 2020
- Gouveia EB, Morales MSA, Gouveia GB, Lourenzi VPM (2007) Ocular toxicity due to 4-aminoquinoline derivatives. *Arq Bras Oftalmol* 70:1046–1051
- Shearer RV, Dubois EL (1967) Ocular changes induced by long-term hydroxychloroquine (plaqueuil) therapy. *Am J Ophthalmol* 64:245–252

7. Lane JCE et al (2020) Risk of hydroxychloroquine alone and in combination with azithromycin in the treatment of rheumatoid arthritis: a multinational, retrospective study. *Lancet Rheumatol* 2:e698–e711. [https://doi.org/10.1016/S2665-9913\(20\)30276-9](https://doi.org/10.1016/S2665-9913(20)30276-9)
8. Vigerust DJ, Shepherd VL (2007) Virus glycosylation: role in virulence and immune interactions. *Trends Microbiol* 15:211–218
9. Wang M, Cao R, Zhang L et al (2020) Remdesivir and chloroquine effectively inhibit the recently emerged novel coronavirus (2019-nCoV) in vitro. *Cell Res* 30:269–271
10. Medicines & Healthcare products Regulatory Agency (1993) *British Pharmacopoeia*, 1st edn. London
11. Tett SE, Cutler DJ, Brown KF (1986) Removal of an endogenous fluorescent compound from urine to allow quantitation of low concentrations of hydroxychloroquine and metabolites by high-performance liquid chromatography. *J Chromatogr Biomed Appl* 383:236
12. Chaulet JF, Mounier C, Soares O, Brazier JL (1991) High-performance liquid chromatographic assay for chloroquine and its two major metabolites, desethylchloroquine and bidesethylchloroquine in biological fluids. *Anal Lett* 24:665–682
13. Morris Raymond G (1986) Estimation of plasma hydroxychloroquine by high-performance liquid chromatography with ultraviolet detection. *J Chromatogr Biomed Appl* 338:422
14. Brocks DR, Pasutto FM, Jamali FJ (1992) Analytical and semi-preparative high performance liquid chromatographic separation and assay of hydroxychloroquine enantiomers. *Chromatogr Biomed* 581:83
15. Wang LZ, Ong RY, Chin TM et al (2012) Method development and validation for rapid quantification of hydroxychloroquine in human blood using liquid chromatography-tandem mass spectrometry. *J Pharm Biomed Anal* 61:86
16. Manjunatha JG, Kumara Swamy BE, Shreenivas MT, Mamatha GP (2012) Selective determination of dopamine in the presence of ascorbic acid using a poly (nicotinic acid) modified carbon paste electrode. *Anal Bioanal Electrochem* 4:225–237
17. Khalil MM, Issa Y, El Sayed GA (2015) Modified carbon paste and polymeric membrane electrodes for determination of hydroxychloroquine sulfate in pharmaceutical preparations and human urine. *RSC Adv*. <https://doi.org/10.1039/C5RA16250E>
18. Manjunatha JG, Kumara Swamy BE, Deraman M, Mamatha GP (2012) Simultaneous voltammetric measurement of ascorbic acid and dopamine at poly (vanillin) modified carbon paste electrode: a cyclic voltammetric study. *Pharma Chem* 4:2489–2497
19. Hareesha N, Manjunatha JG, Amrutha BM, Pushpanjali PA, Charithra MM, Prarith NS (2021) Electrochemical analysis of indigo carmine in food and water samples using poly (glutamic acid) layered multi-walled carbon nanotube paste electrode. *J Electron Mater* 50:1230–1238. <https://doi.org/10.1007/s11664-020-08616-7>
20. Pushpanjali PA, Manjunatha JG, Amrutha BM, Hareesha N (2020) Development of carbon nanotube-based polymer-modified electrochemical sensor for the voltammetric study of curcumin. *Mater Res Innov* 25:412–420. <https://doi.org/10.1080/14328917.2020.1842589>
21. Manjunatha JG (2016) Poly (Nigrosine) modified electrochemical sensor for the determination of dopamine and uric acid: a cyclic voltammetric study. *Int J ChemTech Res* 9:136–146
22. Adimule V, Revaigh MG, Adarsha HJ (2020) Synthesis and fabrication of Y-Doped ZnO nanoparticles and their application as a gas sensor for the detection of ammonia. *J Mater Eng Perform* 29:4586–4596. <https://doi.org/10.1007/s11665-020-04979-4>
23. Ganesh PS, Shimoga G, Lee S, Kim S, Ebenso EE (2021) Interference free simultaneous detection of dihydroxy benzene isomers at cost-effective and reliable celestine blue modified glassy carbon electrode. *Chem Sel* 6:2379–2386. <https://doi.org/10.1002/slct.202100131>
24. Adimule V, Nandi SS, Yallur BC, Bhowmik D, Jagadeesha AH (2021) Optical, structural and Photoluminescence properties of Gd x SrO: CdO nanostructures synthesized by co precipitation method. *J Fluoresc* 31:487–499. <https://doi.org/10.1007/s10895-021-02683-7>
25. Adimule V, Revaiah R, Nandi S, Jagadeesha A (2020) Synthesis, characterization of Cr Doped TeO₂ nano structures and its application as EGFET PH sensor. *Electroanalysis* 33:579–590. <https://doi.org/10.1002/elan.202060329>
26. Hareesha N, Manjunatha JG, Pushpanjali PA et al (2021) Electrochemical sensing of antibiotic drug amoxicillin in the presence of dopamine at simple and selective carbon paste electrode activated with cetyltrimethylammonium bromide surfactant. *Monatsh Chem*. <https://doi.org/10.1007/s00706-021-02870-z>
27. Gururaj KJ, Swamy BEK, Sánchez JPM, Li X, Sharma SC, Lee SL (2020) Electrochemical and quantum chemical studies of cetylpyridinium bromide modified carbon electrode interface for sensor applications. *J Mol Liq* 315:113719. <https://doi.org/10.1016/j.molliq.2020.113719>
28. Shashanka R, Taslimi P, Karaoglanli AC, Uzun O, Alp E, Jayaprakash GK (2021) Photocatalytic degradation of Rhodamine B (RhB) dye in waste water and enzymatic inhibition study using cauliflower shaped ZnO nanoparticles synthesized by a novel One-pot green synthesis method. *Arab J Chem* 14:103180. <https://doi.org/10.1016/j.arabjc.2021.103180>
29. Jayaprakash GK, Kumara Swamy BE, Sharma SC, Santoyo Flores JJ (2020) Analyzing electron transfer properties of ferrocene in gasoline by cyclic voltammetry and theoretical methods. *Microchem J* 158:105116. <https://doi.org/10.1016/j.microc.2020.105116>
30. Rao S, Suhas R, Mahadevaswamy M, Pradeep Kumar CB, Gururaj KJ, Sowmyashree AS, Shwetha K, Aravinda T, Sandeep K (2021) Experimental and DFT explorations of tert-butyl(1-(2-(4-nitrobenzylidene)-hydrazinyl)-1-oxopropan-2-yl)-carbamate on CRCA metal in 1M HCl solution. *Result Surf Interface* 5:100023. <https://doi.org/10.1016/j.rsufri.2021.100023>
31. Hai Yen Pham T, Trang Mai T, Anh Nguyen H, Thi Thu HC, Thi Thu HV, Quoc HL (2021) Voltammetric determination of amoxicillin using a reduced graphite oxide nanosheet electrode. *J Anal Methods Chem*. <https://doi.org/10.1155/2021/882345>
32. Manjunatha JG, Swamy BEK, Gilbert O, Mamatha GP, Sherigara BS (2010) Sensitive voltammetric determination of dopamine at salicylic acid and TX-100, SDS, CTAB modified carbon paste electrode. *Int J Electrochem Sci* 5:682–695
33. Hareesha N, Manjunatha JG, Amrutha BM, Sreeharsha N, Basheeruddin Asdaq SM, Anwer MK (2021) A fast and selective electrochemical detection of vanillin in food samples on the surface of poly(glutamic acid) functionalized multiwalled carbon nanotubes and graphite composite paste sensor. *Colloids Surf A* 626:127042. <https://doi.org/10.1016/j.colsurfa.2021.127042>
34. Manjunatha JG (2020) A surfactant enhanced graphene paste electrode as an effective electrochemical sensor for the sensitive and simultaneous determination of catechol and resorcinol. *Chem Data Coll* 25:100331. <https://doi.org/10.1016/j.cdc.2019.100331>
35. Tigari G, Manjunatha JG (2020) Poly(glutamine) film-coated carbon nanotube paste electrode for the determination of curcumin with vanillin: an electroanalytical approach. *Monatsh Chem* 151:1681–1688. <https://doi.org/10.1007/s00706-020-02700-8>
36. Adimule V, Nandi SS, Jagadeesha Gowda AH (2021) Enhanced power conversion efficiency of the P3BT (poly-3-butyl Thiophene) doped nanocomposites of Gd-TiO₃ as working electrode. Springer, New York. https://doi.org/10.1007/978-3-030-69925-3_6
37. Adimule V, Bowmik D, Adarsha HJ (2020) A facile synthesis of Cr doped WO₃ nanocomposites and its effect in enhanced current-voltage and impedance characteristics of thin films. *Lett Mater* 10:481–485

38. Adimule V, Yallur BC, Sharma K (2021) Studies on crystal structure, morphology, optical and photoluminescence properties of flake-like Sb doped Y_2O_3 nanostructures. *J Opt*. <https://doi.org/10.1007/s12596-021-00746-3>
39. Shashanka R (2021) Investigation of optical and thermal properties of CuO and ZnO nanoparticles prepared by Crocus Sativus (Saffron) flower extract. *J Iran Chem Soc* 18:415–427. <https://doi.org/10.1007/s13738-020-02037-3>
40. Shashanka R, Esgin H, Yilmaz VM, Caglar Y (2020) Fabrication and characterization of green synthesized ZnO nanoparticle based dye-sensitized solar cell. *J Sci Adv Mater Device* 5:185–191
41. Shashanka R, Volkan MY, Abdullah CK, Orhan U (2020) Investigation of activation energy and antibacterial activity of CuO nanorods prepared by Tilia Tomentosa (Ihlamur) leaves. *Moroccan J Chem* 8:497–509
42. Adimule V, Nandi SS, Yallur BC, Bhowmik D, Jagadeesha AH (2021) Enhanced photoluminescence properties of Gd (x–1) Sr x O: CdO nanocores and their study of optical, structural, and morphological characteristics. *Mater Today Chem* 20:100438. <https://doi.org/10.1016/j.mtchem.2021.100438>
43. Adimule V, Yallur BC, Bhowmik D, Jagadeesha AH (2021) Morphology, structural and photoluminescence properties of shaping triple semiconductor $YxCoO:ZrO_2$ nanostructures. *J Mater Sci Mater Electron* 32:12164–12181. <https://doi.org/10.1007/s10854-021-05845-2>
44. Adimule V, Yallur BC, Kamat V, Krishna PM (2021) Characterization studies of novel series of cobalt (II), nickel (II) and copper (II) complexes: DNA binding and antibacterial activity. *J Pharm Investig* 51:347–359. <https://doi.org/10.1007/s40005-021-00524-0>
45. Pushpanjali PA, Manjunatha JG, Hareesha N, Amrutha BM, Raril C, Zeid AA, Amer MA, Anup P (2022) Fabrication of poly(L-aspartic acid) layer on graphene nanoplatelets paste electrode for riboflavin sensing. *Mater Chem Phys* 276:125392. <https://doi.org/10.1016/j.matchemphys.2021.125392>
46. Hareesha N, Manjunatha JG (2021) Electro-oxidation of formoterol fumarate on the surface of novel poly(thiazole yellow-G) layered multi-walled carbon nanotube paste electrode. *Sci Rep* 11:12797. <https://doi.org/10.1038/s41598-021-92099-x>
47. Ali Y, Alam AU, Howlader MMR (2020) Fabrication of highly sensitive Bisphenol A electrochemical sensor amplified with chemically modified multiwall carbon nanotubes and cyclodextrin. *Sens Actuators B* 320:128319
48. Jaise MG, Beena M (2021) Cyclodextrin-mediated gold nanoparticles as multisensing probe for the selective detection of hydroxychloroquine drug. *Korean J Chem Eng* 38:624–634. <https://doi.org/10.1007/s11814-020-0719-7>
49. Ganesh PS, Shimoga G, Lee SH, Kim SY, Ebenso EE (2021) Simultaneous electrochemical sensing of dihydroxy benzene isomers at cost-effective allura red polymeric film modified glassy carbon electrode. *J Anal Sci Technol* 12:20. <https://doi.org/10.1186/s40543-021-00270-w>
50. Ganesh PS, Swamy BEK (2015) Simultaneous electroanalysis of norepinephrine, ascorbic acid and uric acid using poly(glutamic acid) modified carbon paste electrode. *J Electroanal Chem* 752:17–24. <https://doi.org/10.1016/j.jelechem.2015.06.002>
51. Patrícia BD, Fernando CV, Geiser GO, Romeu CR-F, Orlando F-F (2014) Square-wave voltammetric determination of hydroxychloroquine in pharmaceutical and synthetic urine samples using a cathodically pre-treated boron-doped diamond electrode. *J Electroanal Chem* 719:19–23
52. Ganesh PS, Swamy BEK, Feyami OE, Ebenso Eno E (2018) Interference free detection of dihydroxybenzene isomers at pyrogallol film coated electrode: a voltammetric method. *J Electroanal Chem* 813:193–199. <https://doi.org/10.1016/j.jelechem.2018.02.018>
53. Teradale AB, Lamani SD, Ganesh PS, Swamy BEK, Das SN (2017) Electrochemical sensor for the determination of paracetamol at carbamazepine film coated carbon paste electrode. *Z Phys Chem* 232:345–358. <https://doi.org/10.1515/zpch-2017-0992>
54. Mahnashi HM, Mahmoud AM, Alkahtani AS, Mohamed ME (2021) Simultaneous electrochemical detection of azithromycin and hydroxychloroquine based on VS2 QDs embedded N, S @graphene aerogel/cCNTs 3D nanostructure. *Microchem J* 163:105925. <https://doi.org/10.1016/j.microc.2021.105925>
55. Jayaprakash GK, Kumara Swamy BE, Rajendrachari S, Sharma SC, Flores-Moreno R (2021) Dual descriptor analysis of cetylpyridinium modified carbon paste electrodes for ascorbic acid sensing applications. *J Mol Liq* 334:116348. <https://doi.org/10.1016/j.molliq.2021.116348>
56. Tigari G, Jamballi GM, Pushpanjali PA, Prinith NS, Ravishankar DK, Siddaraju G (2021) Poly (DL-valine) electro-polymerized carbon nanotube paste sensor for determination of antihistamine drug cetirizine. *J Electrochem Sci Eng* 11:27–38. <https://doi.org/10.5599/jese.934>
57. Khalil MM, Issa YM, El Sayed GA (2015) Development of a new coated graphite electrode for hydroxychloroquine sulfate determination in pharmaceutical preparations and human urine. *Int J Adv Res* 3:592–603

Publisher's Note Springer Nature remains neutral with regard to jurisdictional claims in published maps and institutional affiliations.